Journal of Solid State Chemistry **145,** 77–87 (1999)
Article ID jssc.1999.8220, available online at http://www.idealibrary.com on IDEAL®

Energetics of Rare Earth Manganese Perovskites $A_{1-x}A'_xMnO_3$ (A = La, Nd, Y and A' = Sr, La) Systems

Christel Laberty and Alexandra Navrotsky

Thermochemistry Facility, Chemistry Annex, Department of Chemical Engineering and Materials Science, University of California at Davis, Davis, California 95616

C. N. R. Rao

Solid State and Structural Chemistry Unit, Indian Institute of Science, Bangalore 560012, India

and

Pierre Alphonse

Laboratoire de Chimie des Matériaux Inorganiques, Université Paul Sabatier Toulouse, 118 Route de Narbonne, 31062 Toulouse Cedex, France

Received September 24, 1998; in revised form February 10, 1999; accepted February 11, 1999

High temperature reaction calorimetry using molten lead borate as solvent has been used to study the thermochemistry of $NdMnO_3$, $YMnO_3$, $La_{1-x}Sr_xMnO_3$ (with $0<x<0.5$), and $Ln_{0.5}Ca_{0.5}MnO_3$ (with Ln = La, Nd, Y). The enthalpies of formation of these multicomponent oxides from their binary constituents have been calculated from the measured enthalpy of drop solution. The energetic stability of the perovskite depends on the size of the A cation. The enthalpy of formation of $YMnO_3$ (smallest A cation) is more endothermic than those of $NdMnO_3$ and $LaMnO_3$. The energetics of the perovskite also depends on the oxidation state of the B site's ions. In the $La_{1-x}Sr_xMnO_3$ system, the energetic stability of the structure increases with the Mn^{4+}/Mn^{3+} ratio. The new values of the enthalpies of oxidations, with reliable standard entropies, were used to plot the phase stability diagram of the lanthanum–manganese–oxygen system in the temperature range 300–1100 K. The $LaMnO_3$/MnO phase boundary evaluated in this study agrees with the one published by Atsumi *et al.* calculated from thermogravimetric and conductivity measurements. © 1999 Academic Press

INTRODUCTION

Perovskite oxides with the general formula ABO_3 have been the subject of many studies because of their good electrical (1), and magnetic (2), and catalytic properties (3). Recently, the discovery of giant magnetoresistence (GMR) in rare earth manganites of the type $A_{1-x}A'_xMnO_3$ (A = rare earth, A' = alkaline earth) has created much interest in understanding the relation between structure and properties of these oxides (1–4). Substitution of La in $LaMnO_3$ by Ca or Sr results in the formation of Mn^{4+} and the effects of tetravalent manganese on structure (5), electrical conductivity (6), and magnetic susceptibility (7) have been investigated extensively. Because of their particular structure and the various oxidation states of manganese, alkaline earth doped $LaMnO_3$ phases can be used as cathode (e.g., Sr-doped $LaMnO_3$) and interconnection materials in solid oxide fuel cells (SOFC) and electrochemical reactors (8–11). However, the materials are often utilized at high temperatures and sometimes in highly reducing atmospheres. To understand the physical properties of these materials and their behavior in SOFC and to be able to describe the chemical stability of the compounds and their reactivity with other materials, values of thermodynamic parameters are needed.

The nonstoichiometry, stability range, and thermodynamic properties of the decomposition reaction of $LaMnO_3$ to form La_2O_3 and MnO (Eq. [1]) have been studied by thermogravimetry (TG) (12), electrical conductivity (13), and solid-electrolyte galvanic cell measurements (14).

$$LaMnO_3 \rightarrow MnO + \tfrac{1}{4}O_2 + \tfrac{1}{2}La_2O_3 \qquad [1]$$

The ΔG^0 of the reversible decomposition reaction of $LaMnO_3$ was determined from the critical partial pressure of oxygen when a sudden weight change occurred (15). Nakamura *et al.* (16) studied the chemical stability range of $LaBO_3$ (B = V, Cr, Mn, Co, Ni) at 1273 K in a reducing atmosphere by thermogravimetry. The ΔG^0_T, ΔH^0_T, and ΔS^0_T for the above reaction were calculated. Utilizing electrical conductivity, Kamegashira *et al.* (17) measured the critical

0022-4596/99 $30.00

P_{O_2} for the decomposition of $LaMnO_3$ in the temperature range 1173–1473 K. The ΔG^0_T, ΔH^0_T, and ΔS^0_T of the decomposition reaction have been reported (17). The EMF method has been used by Sreedharan *et al.* (18) to measure the ΔG^0_T of formation of $LaMnO_3$ from La_2O_3 and MnO.

In all the above studies, ΔH^0_T and ΔS^0_T were determined simultaneously from the temperature dependence of ΔG^0. It is difficult to assess the uncertainty in these values. Apart from some preliminary measurements in our laboratory (19), no direct determination of enthalpies of formation of doped manganites has been reported. Thus, the purpose of the present study was to directly determine thermochemical parameters for the $La_{1-x}Sr_xMnO_3$ (with $0 < x < 0.5$) and $Ln_{0.5}Ca_{0.5}MnO_3$ (with Ln = La, Nd, Y) systems, using transposed temperature drop calorimetry and high temperature drop solution calorimetry. The thermochemical data are discussed in terms of the average size of the A cations, the oxidation state of manganese, and the tolerance factor. The new values of the enthalpy of formation of $LaMnO_3$ have been combined with reliable standard entropies to construct a phase stability diagram for the La–Mn–O system in the temperature range 300–1100 K. The calculated phase boundary between $LaMnO_3$ and MnO agrees well with the one published in the literature determined from weight change and conductivity measurements. This agreement confirms the accuracy and consistency of the calorimetric experiments. The thermochemical data reported for the other materials, which have not been measured before, are thus also very likely to be reliable.

EXPERIMENTAL METHODS

Sample Preparation

These compounds were prepared by heating stoichiometric mixtures of simple oxides (La_2O_3, Y_2O_3, Nd_2O_3) with carbonates ($CaCO_3$, $SrCO_3$, $MnCO_3$) at 1223 K for 12 h. The powder thus obtained was ground and further heated for 24 h at the same temperature. The synthesis protocol is given elsewhere (13–18).

Characterization

Powder diffraction patterns were obtained with a Scintag PAD V automated diffractometer using monochromatic Cu$K\alpha_1$ radiation (d = 1.5409 Å). For qualitative identification of the phases, the patterns were taken from $20^\circ < 2\theta < 70^\circ$ with a scan rate of 1° (2θ/min). The scan rate used to obtain X-ray patterns for precision cell constant determination was 0.25° (2θ/min). Sodium chloride was used as an internal standard and a least squares refinement program was used to determine cell parameters.

The Mn^{4+} contents of substituted samples were determined by redox titration using standard ferrous sulfate and potassium permanganate (20, 21). The oxygen stoichiometry for each composition was evaluated from a programmed temperature reduction cycle using a thermobalance (Cahn system 113). Samples (200 mg) were loaded in a TGA bucket and outgassed under vacuum for 1 h at room temperature. The apparatus was then filled with Ar. During the experiment, a constant Ar flow rate of 40 cc/sec was maintained. The temperature was increased to 1273 K at a rate of 5 K/min and held at 1273 K for 1 h. The exhaust gas mixture was analyzed by both mass spectrometry and gas chromatography. The latter technique allows the evaluation of the oxygen stoichiometry of the sample whereas mass spectrometry shows the nature of any compounds adsorbed on the surface.

Calorimetry

High transposed temperature drop calorimetry and drop solution calorimetry were performed on a Tian–Calvet type microcalorimeter which is described elsewhere (22–24). The calibration factor of the calorimeter was obtained by dropping pellets (of known mass and heat content) of alumina (Aldrich, 99.99%) which had been fully converted to the corundum phase by heating for 24 h at 1773 K. Transposed temperature drop calorimetry was performed by dropping a sample pellet into an empty platinum crucible in the calorimeter. The measured heat effect included the heat content of the sample from room temperature to 977 K and the heat associated with any reaction (oxidation, reduction, H_2O or CO_2 loss) which occurred in the calorimeter. Drop solution calorimetry was performed by dropping a sample pellet into lead borate solvent ($2PbO–B_2O_3$) in a platinum crucible in the calorimeter. The total heat effect included the heat of solution and the heat effect measured by transposed temperature drop calorimetry.

In this paper, when we compare the stability of different compounds, we refer to the enthalpy or free energy of the multicomponent oxide with respect to component binary oxides. For example, the stability of $LaMnO_3$ is the stability with respect to La_2O_3 and Mn_2O_3.

RESULTS AND DISCUSSION

X-Ray Diffraction

The cell parameters are shown in Table 1. All of the analyzed samples were single phases. In the system $La_{1-x}Sr_xMnO_3$, the unit cell is rhombohedral for $x < 0.5$ and orthorhombic for $x = 0.5$. In the system $Ln_{0.5}Ca_{0.5}MnO_3$, the unit cell is orthorhombic for Ln = Nd, Y. The Mn^{4+} content of the various samples and the average radius of the A-site cations (in ninefold coordination (25)) are also listed in Table 1. In $La_{1-x}Sr_xMnO_3$, incorporation of Sr progressively increases the Mn^{4+}/Mn^{3+} ratio. The

TABLE 1
Structural Properties of Manganites

Compound	$\%Mn^{4+a}$	$\langle r_A \rangle^b$ (Å)	Structure	Lattice (Å)
$LaMnO_3$	—	1.216	Orthorhombic	$a = 5.514$ $b = 5.554$ $c = 7.765$
$NdMnO_3$	—	1.163	Orthorhombic	$a = 5.409$ $b = 5.432$ $c = 7.625$
$YMnO_3$	—	1.075	Cubic	$a = 7.754$
$La_{0.9}Sr_{0.1}MnO_3$	27	1.225	Rhombohedral	5.506
$La_{0.7}Sr_{0.3}MnO_3$	37	1.244	Rhombohedral	5.440
$La_{0.5}Sr_{0.5}MnO_3$	46	1.263	Orthorhombic	$a = 5.442$ $b = 7.698$ $c = 5.479$
$La_{0.5}Ca_{0.5}MnO_3$	44	1.198	Orthorhombic	$a = 5.418$ $b = 7.639$ $c = 5.427$
$Nd_{0.5}Ca_{0.5}MnO_3$	52	1.171	Orthorhombic	$a = 5.384$ $b = 7.608$ $c = 5.406$
$Y_{0.5}Ca_{0.5}MnO_3$	43	1.127	Orthorhombic	$a = 5.305$ $b = 7.445$ $c = 5.495$

[a] From redox titrations.
[b] Average size of the *A*-site cation.

Mn^{4+} contents of $LaMnO_3$, $NdMnO_3$, and $YMnO_3$ were evaluated from TG analyses.

Thermal Analyses

The weight of the $La_{0.5}Sr_{0.5}MnO_3$, $Y_{0.5}Ca_{0.5}MnO_3$ and $Nd_{0.5}Ca_{0.5}MnO_3$, and $LaMnO_3$ and $NdMnO_3$, and $YMnO_3$ samples did not change when heated in argon up to 1273 K. This strongly suggests that the samples are stoichiometric in terms of Mn/O = 1/3. For $La_{0.5}Ca_{0.5}MnO_3$, the weight loss was 0.4% and occurred in two steps: 0.3% around 673 K and 0.1% around 773 K. Gas chromatographic analyses suggest that the oxide is stoichiometric because no evolved oxygen gas was detected. In order to identify the species adsorbed on the surface, mass spectrometry was employed. The peaks at 773 and 673 K correspond to CO_2 and H_2O masses, respectively. Carbonate decomposition and hydroxyl desorption from the surface of the sample are thus inferred. For $La_{0.7}Sr_{0.3}MnO_3$ samples, the total weight loss was 0.4% and took place in three steps: 0.25% around 573 K, 0.1% around 773 K, and 0.05% at 873 K. As in $La_{0.5}Ca_{0.5}MnO_3$, no oxygen was detected by gas chromatography, which indicates that the oxide is stoichiometric. Mass spectrometry shows that the first two steps correspond to hydroxyl decomposition and the last to carbonate decomposition. For $La_{0.9}Sr_{0.1}MnO_3$, the weight loss was 0.5% and occurred in three steps: 0.2% around 573 K, 0.1% around 823 K, and 0.2% around 973 K. Gas chromatography indicates that this oxide is nonstoichiometric because oxygen evolution was detected at 923 K. Mass spectrometry shows that the first two steps correspond to hydroxyl decomposition and the last one to carbonate decomposition. Mass spectrometry and gas chromatography together indicate that the last step is a combination of carbonate desorption (923 K) and oxygen loss 973 K). The integration of the variation of O_2 concentration in flowing gas with time permits the quantification of the oxygen deficiency. The compositions of the samples studied are listed in Tables 2 and 3.

Calorimetry

Calorimetric data for the measured enthalpy of transposed temperature drop experiments are presented in Table 2. The X-ray patterns were checked after the first and the second drops to confirm that there were no structural changes during the drop of the sample. For $Nd_{0.5}Ca_{0.5}MnO_3$, $Y_{0.5}Ca_{0.5}MnO_3$, $La_{0.5}Sr_{0.5}MnO_3$, $LaMnO_3$, $NdMnO_3$, and $YMnO_3$, the values of the measured enthalpy for the first and the second drops are the same within experimental error. However, the $La_{0.7}Sr_{0.3}MnO_3$, $La_{0.9}Sr_{0.1}MnO_3$, and $La_{0.5}Ca_{0.5}MnO_3$, the measured heat effect for the second drop is systematically less endothermic. This result can be attributed to the presence of hydroxyl groups and carbonate adsorbed on the surface of these samples (shown previously by TG). The measured enthalpy of transposed temperature drop represents the sum of the heat content of the sample plus the heat absorbed when the hydroxyl and/or carbonate desorption occurs. This result is similar to the observation by McHale *et al.* (26) on aluminum oxides showing that the extra water increases the apparent heat content of the sample.

To a first approximation, the heat content of a multicomponent oxide can be calculated as a sum of binary oxide heat contents (Kopp–Neumann rule, see Table 4), since $H_{977}-H_{298}$ for the simple oxides (La_2O_3, CaO, Mn_2O_3, MnO_2, SrO, Nd_2O_3, Y_2O_3) are known. For example, for the case of $La_{1-x}Sr_xMnO_3$,

$$La_{1-x}Sr_xMnO_3 \rightarrow (1-x)/2\ La_2O_3 + xSrO + (1/2-x/2)Mn_2O_3 + xMnO_2, \quad [2]$$

the heat content would be equal to the heat content of La_2O_3, SrO, Mn_2O_3, and MnO_2, taken in the indicated proportions. The enthalpies measured for the second drop match the heat content calculated from the component oxides. This agreement confirms that during the first drop the heat measured corresponds to the heat content of the

TABLE 2
Summary of Sample Characterization and Data Obtained by Transposed Temperature Drop Calorimetry

Compounds	M[a] (g/mol)	x[b]	y[c]	M[d] corrected (g/mol)	ΔH_{ttd1} (kJ/g)	ΔH_{ttd1} (kJ/mol)	Correction for water (kJ/mol)[g]	Correction for carbon dioxide (kJ/mol)[h]	ΔH_{ttd1c} (kJ/mol)[i]	ΔH_{ttd2} (kJ/g)[j]	ΔH_{ttd2} (kJ/mol)[k]
$LaMnO_3$	241.85	—	—	241.85	0.34[e]	82.62[f]	—	—	**82.8±1.2**	0.34	**82.6[l]±2.2[m]**
$YMnO_3$	191.85	—	—	191.85	0.33	84.56	—	—	**83.8±1.2**	0.33	**84.6±1.2**
$NdMnO_3$	121.57	—	—	247.18	0.43	84.25	—	—	**84.1±1.4**	0.43	**84.2±1.4**
$La_{0.9}Sr_{0.1}MnO_{3.01}$	236.98	0.039	0.010	238.15	0.37	87.45	2.77	1.69	**82.9±1.54**	0.35	**82.3±2.5**
$La_{0.7}Sr_{0.3}MnO_3$	226.52	0.044	0.003	227.43	0.38	85.78	3.08	0.42	**82.3±0.9**	0.36	**82.0±3.1**
$La_{0.5}Sr_{0.5}MnO_3$	216.18	—	—	216.18	0.37	81.18	—	—	**81.2±3.9**	0.38	**81.9±2.1**
$La_{0.5}Ca_{0.5}MnO_3$	193.13	0.032	0.004	193.90	0.45	86.77	2.25	0.48	**84.0±1.1**	0.43	**82.8±2.5**
$Y_{0.5}Ca_{0.5}MnO_3$	167.41	—	—	167.41	0.51	84.96	—	—	**84.9±1.3**	0.50	**84.5±1.9**
$Nd_{0.5}Ca_{0.5}MnO_3$	195.07	—	—	195.08	0.43	84.12	—	—	**84.1±2.1**	0.43	**84.1±1.4**

[a] M, molecular mass of $Ln_{1-x}A_xMnO_3$ (with A = Ca, Sr and Ln = La, Y, Nd).
[b] x, water content estimated from TGA analyses (per unit formula).
[c] y, CO_2 content estimated from TGA analyses (per unit formula).
[d] M corrected, molecular mass of $Ln_{1-x}A_xMnO_3$, xH_2O, yCO_2 (with A = Ca, Sr and Ln = La, Y, Nd).
[e] Enthalpy of transposed temperature drop, measured by transposed temperature drop calorimetry, first drop.
[f] Enthalpy of transposed temperature drop, calculated from transposed temperature drop calorimetry using molecular weight, M corrected, based on chemical analysis.
[g] Water correction assuming physisorbed water, 70.09 kJ/mol heat content.
[h] Carbon dioxide correction assuming chemisorbed CO_2 on strontium (108.9 kJ/mol) and calcium (163.5 kJ/mol).
[i] Corrected enthalpy of transposed temperature drop (heat content plus dehydroxylation/removing adsorbed CO_2).
[j] Enthalpy of transposed temperature drop, measured by transposed temperature drop calorimetry, second drop.
[k] Calculated from transposed temperature drop calorimetry second drop using molecular weight, M, based on chemical analysis.
[l] Average based on six experiments.
[m] Uncertainty is two standard deviations of the mean.

sample plus other reactions in the calorimeter, but that in the second drop, no further reactions occur.

The TG analyses (see above) suggest that the water in the samples consists predominantly of hydroxyl at the surface, which is desorbed at relatively high temperature (673 K). However, to our knowledge, no data concerning the strength of adsorption of hydroxyl on the perovskite surface are available. Therefore, to a first approximation, the heat of adsorption of the physisorbed surface water is given by the heat of condensation of gaseous water. When the sample is dropped from room temperature into the hot calorimeter, the heat of desorption is given by the heat content of water, 70.09 kJ/mol, according to the equation of Robie and Hemingway for the reaction (27):

$$H_2O\ (\text{liquid, 298 K}) \longrightarrow H_2O\ (\text{gas, 979 K}). \quad [3]$$

Mass spectrometry suggests the presence of carbonate on the surface of $La_{0.5}Ca_{0.5}MnO_3$, $La_{0.7}Sr_{0.3}MnO_3$, and $La_{0.9}Sr_{0.1}MnO_3$. At the surface of the perovskite, at least two types of CO_2 adsorption can occur: physisorbed CO_2 (adsorption of CO_2 on the oxide surface) and chemisorbed CO_2 (interaction of CO_2 with the surface to form carbonate groups). The TG analyses suggest that the samples contain predominantly chemisorbed CO_2 at the surface, which decomposes only at high temperature (873 K). Previous thermodynamic studies show that $MnCO_3$ is less stable in enthalpy than $CaCO_3$ and $SrCO_3$ (31). The correction for carbonate was done assuming that the CO_2 is mainly chemisorbed on strontium or calcium. Accordingly, the heat of adsorption of the CO_2 was estimated to be the heat of formation of the corresponding carbonate at 977 K. When the sample is dropped from room temperature into the hot calorimeter, the heat of desorption is given by the reverse of the heat of formation of carbonate from the oxides at 977 K:

$$MCO_3(\text{s, 977 K}) \rightarrow MO(\text{s, 977 K}) + CO_2(\text{g, 977 K}). \quad [4]$$

This enthalpy is 108.9 kJ/mol for $CaCO_3$ and 163.4 kJ/mol for $SrCO_3$.

Thus, the corrected enthalpy of the oxide measured by drop solution calorimetry or transposed temperature drop calorimetry is: $\Delta H = \Delta H_{(\text{ttdl or ds})} - x\Delta H_{H_2O} - y\Delta H_{CO2}$, where $\Delta H_{(\text{ds or ttd})}$ is the measured enthalpy using either the first transposed temperature drop or the drop solution, respectively, x is the quantity of water determined by TG analyses, ΔH_{H2O} is the heat content of water, 70.09 kJ/mol, y is the quantity of adsorbed CO_2 determined by TGA analyses, and ΔH_{CO2} is the heat of decomposition of the corresponding carbonate.

TABLE 3
Summary of Sample Characterization and Data Obtained by Drop Solution Calorimetry

Compounds	M (g/mol)[a]	x[b]	y[c]	M[d] corrected (g/mol)	ΔH_{ds} (kJ/g)	ΔH_{ds} (kJ/mol)	Correction for water (kJ/mol)[g]	Correction for carbon dioxide (kJ/mol)[h]	ΔH_{ds} (kJ/mol)[k]
$LaMnO_3$	241.85	—	—	241.85	0.51(e)	124.53(f)	—	—	**126.5[i]±2.1[j]**
$NdMnO_3$	191.85	—	—	191.85	0.49	121.57	—	—	**121.6±1.9**
$YMnO_3$	121.57	—	—	121.57	0.87	115.28	—	—	**115.2±2.1**
$La_{0.9}Sr_{0.1}MnO_{3.01}$	236.98	0.039	0.010	238.15	0.502	119.69	2.77	1.69	**115.2±1.9**
$La_{0.7}Sr_{0.3}MnO_3$	226.52	0.044	0.003	227.43	0.501	114.02	3.08	0.42	**110.5±0.5**
$La_{0.5}Sr_{0.5}MnO_3$	216.18	—	—	216.18	0.487	105.3	—	—	**105.2±2.2**
$La_{0.5}Ca_{0.5}MnO_3$	193.13	0.032	0.004	193.90	0.582	112.96	2.25	0.48	**110.2±2.9**
$Y_{0.5}Ca_{0.5}MnO_3$	167.41	—	—	167.41	0.610	102.23	—	—	**102.2±2.5**
$Nd_{0.5}Ca_{0.5}MnO_3$	195.07	—	—	195.08	0.541	105.7	—	—	**105.7±2.8**

[a] M, molecular mass of $Ln_{1-x}A_xMnO_3$ (with A = Ca, Sr and Ln = La, Y, Nd).
[b] x, water content estimated from TGA analyses (per unit formula).
[c] y, CO_2 content estimated from TGA analyses (per unit formula).
[d] M corrected, molecular mass of $Ln_{1-x}A_xMnO_3$, xH_2O, yCO_2 (with A = Ca, Sr and Ln = La, Y, Nd).
[e] Enthalpy of drop solution, measured by drop solution calorimetry.
[f] Enthalpy of drop solution, calculated from drop solution calorimetry using molecular weight, M corrected, based on chemical analysis.
[g] Water correction assuming physisorbed water, 70.09 kJ/mol heat content.
[h] Carbon dioxide correction assuming chemisorbed CO_2 on strontium (108.9 kJ mol) and calcium (163.5 kJ/mol).
[i] Corrected enthalpy of drop solution (heat content plus removing adsorbed CO_2/dehydroxylation).
[j] Average based on six experiments.
[k] Uncertainty is two standard deviations of the mean.

The measured enthalpies and the corrected enthalpies for water and carbonate are given in Tables 2 and 3. The heat effects of the first drop corrected for water and carbonates desorption are identical to the heat effect of the second drop, within experimental error. This agreement between corrected first drop, second drop, and Kopp–Neumann values supports the appropriateness of these corrections terms.

ENTHALPIES OF FORMATION FROM THE OXIDES

The enthalpies of formation of $LaMnO_3$, $YMnO_3$, $NdMnO_3$, $La_{1-x}Sr_xMnO_3$, and $Ln_{0.5}Ca_{0.5}MnO_3$ from the binary oxide at 298 K have been calculated from the measured values of the enthalpies of drop solution of these compounds and the enthalpy of solution at 977 K of the component oxides. An example of the thermodynamic cycle used is shown for $La_{1-x}Sr_xMnO_3$.

$$\Delta H_5 \quad (1-x)/2\ La_2O_3\ (\text{sol, 977 K}) + x\text{SrO}\ (\text{sol, 977 K}) + 1/2\ Mn_2O_3\ (\text{sol, 977 K}) + x/4O_2\ (\text{g, 977 K}) \rightarrow La_{1-x}Sr_xMnO_3\ (\text{s, 298 K}) \quad [5]$$

$$\Delta H_6 \quad (1-x)/2\ La_2O_3\ (\text{s, 298 K}) \rightarrow (1-x)/2\ La_2O_3\ (\text{sol, 977 K}) \quad [6]$$

$$\Delta H_7 \quad x\text{SrO}\ (\text{s, 298 K}) \rightarrow x\text{SrO}\ (\text{sol, 977 K}) \quad [7]$$

$$\Delta H_8 \quad 1/2\ Mn_2O_3\ (\text{s, 298 K}) \rightarrow 1/2\ Mn_2O_3\ (\text{sol, 977 K}) \quad [8]$$

$$\Delta H_9 \quad (x/4)\ O_2\ (\text{g, 298 K}) \rightarrow (x/4)\ O_2\ (\text{g, 977 K}) \quad [9]$$

$$\Delta H_{10} \quad (1-x)/2\ La_2O_3\ (\text{s, 298 K}) + x\text{SrO}\ (\text{s, 298 K}) + 1/2\ Mn_2O_3\ (\text{s, 298 K}) + x/4\ O_2\ (\text{g, 298 K}) \rightarrow La_{1-x}Sr_xMnO_3\ (\text{s, 298 K}) \quad [10]$$

In this equation, $\Delta H_{10} = \Delta H_5 + \Delta H_6 + \Delta H_7 + \Delta H_8 + \Delta H_9$; ΔH_5 is the measured enthalpy of drop solution (Table 3). The enthalpies of drop solution at 298 K of La_2O_3, SrO, and Mn_2O_3 are ΔH_6, ΔH_7, and ΔH_8, respectively. The enthalpies of drop solution of these compounds represent the sum of the enthalpies of solution plus the heat content measured between 298 and 977 K. The values of the heat content of La_2O_3, SrO, and Mn_2O_3 are from Robie and Hemingway (27). The heats of solution of La_2O_3 and SrO are from Bularzik *et al.* (28), of Nd_2O_3 is from Takayama-Muromachi *et al.* (29), of Y_2O_3 is from Zhou *et al.* (30) and for CaO from Chai *et al.* (31). The calculated enthalpies of formation of perovskite from the components' binary oxides are reported in Table 5.

TABLE 4
Measured Heat Content and Calculated Heat Content Using the Kopp–Neumann Rule

Composition	Heat content from literature (kJ/mol)	Heat content calculated from the Kopp–Neumann rule (kJ/mol)	$\Delta H_{ttd1,cor}$[e] (kJ/mol)	ΔH_{ttd2}[d] (kJ/mol)
La_2O_3	82.9[a]	—	—	—
CaO	35.6[a]	—	—	—
Mn_2O_3	82.8[b]	—	—	—
SrO	32.2[b]	—	—	—
Nd_2O_3	88.7[a]	—	—	—
Y_2O_3	85.9[a]	—	—	—
MnO_2	48.0[a]	—	—	—
$LaMnO_3$	—	82.8	82.8 ± 1.2	82.6 ± 2.2
$NdMnO_3$	—	85.7	84.1 ± 1.4	84.6 ± 1.2
$YMnO_3$	—	84.3	83.8 ± 1.2	84.2 ± 1.4
$La_{0.5}Ca_{0.5}MnO_3$	—	83.3	84.0 ± 1.1	82.8 ± 2.5
$Nd_{0.5}Ca_{0.5}MnO_3$	—	83.9	84.1 ± 2.1	84.1 ± 1.4
$Y_{0.5}Ca_{0.5}MnO_3$	—	84.7	84.9 ± 1.3	84.5 ± 1.9
$La_{0.5}Sr_{0.5}MnO_3$	—	81.6	81.2 ± 3.9	81.9 ± 2.1
$La_{0.7}Sr_{0.3}MnO_3$	—	82.1	82.3 ± 0.9	82.0 ± 3.1
$La_{0.9}Sr_{0.1}MnO_3$	—	82.6	82.9 ± 1.5	82.3 ± 2.5

[a] Values from Robie and Hemingway (27).
[b] Values from Fritsch and Navrotsky (35).
[c] $\Delta H_{ttd1,cor}$, Enthalpy of transposed temperature drop, measured by transposed temperature drop calorimetry, first drop corrected for CO_2 and H_2O.
[d] ΔH_{ttd2}, Enthalpy of transposed temperature drop, measured by transposed temperature drop calorimetry, second drop.

DISCUSSION OF ENERGETIC TRENDS

The stability of the perovskite structure depends on the relative sizes of the *A* and *B* ions as well as on the electronic configuration of the *B* site ions (21). The size factor is expressed by the tolerance factor, *t*,

$$t = \frac{r_A + r_O}{\sqrt{2}(r_B + r_A)}, \qquad [11]$$

where r_A, r_B and r_O are the ionic radii of the *A*, *B*, and *O* ions taken from Shannon (25). Takayama-Muromachi and Navrotsky (32) have shown that the heat of formation of perovskite compounds from the oxides becomes less negative as *t* deviates from unity. Accordingly, the variation of the enthalpy of formation as a function of $1 - t$ is presented in Fig. 1. The enthalpies of formation are shifted to more positive values with $1 - t$. A comparison of the enthalpies of formation of $A_{0.5}Ca_{0.5}MnO_3$ compounds shows that the value is more endothermic for Y than for Nd and La. The diminished stability of $Y_{0.5}Ca_{0.5}MnO_3$ is probably related to the relatively small size of the Y^{3+} cation in the central site.

The symmetry of the $La_{1-x}Sr_xMnO_3$ structure depends on the Mn^{4+} content. When strontium substitutes for lanthanum, the Mn^{4+} content increases and the structure changes from rhombohedral to cubic (33). Studies on manganese oxides have shown the influence of the oxidation state of manganese on the energetics (34–35). In order to separate effects of the oxidation reaction (O_2 involved in the reaction, ΔH_{10}) from those of the substitution of La for Sr, a second thermodynamic cycle was used. The formation of perovskite can be written to incorporate Mn_2O_3 and MnO_2 rather than Mn_2O_3 and gaseous O_2. In this case, the

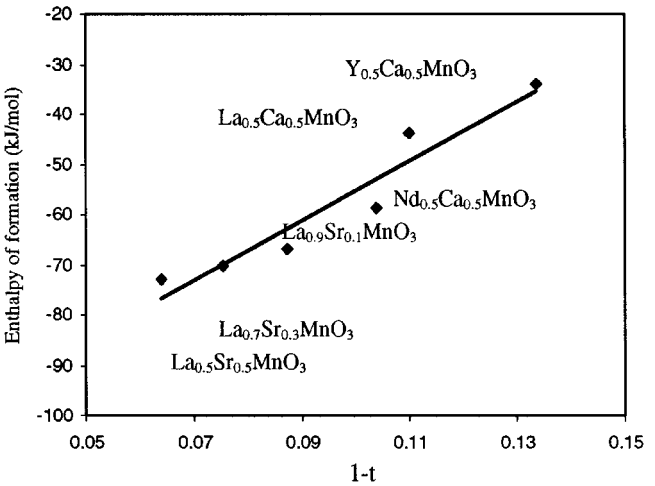

FIG. 1. Formation reaction: $x/4O_2 + xAO + (1-x)/2Ln_2O_3 + 1/2Mn_2O_3 \rightarrow Ln_{1-x}A_xMnO_3$. Enthalpy of formation of manganite perovskites from oxides as a function of $1 - t$ where t = tolerance factor. (□) Formation from AO, Ln_2O_3, Mn_2O_3, and O_2; (■) formation from AO, Ln_2O_3, Mn_2O_3, and MnO_2.

TABLE 5
Enthalpies of Formation from the Oxides and Elements of the Studied Compounds at 298 K

Compounds	ΔH_{10} (kJ/mol)[a]	ΔH_{17} (kJ/mol)[b]	$\Delta H_{elements}$ (kJ/mol)
$LaMnO_3$	-74.8 ± 2.5	-74.8 ± 2.5	-1451.1 ± 2.5
$NdMnO_3$	-48.5 ± 1.8	-48.5 ± 1.8	-1431.9 ± 1.8
$YMnO_3$	-29.8 ± 2.1	-29.8 ± 2.1	-1461.9 ± 2.1
$La_{0.5}Ca_{0.5}MnO_3$	-56.6 ± 6.3	-15.4 ± 2.9	-1302.1 ± 6.3
$Nd_{0.5}Ca_{0.5}MnO_3$	-41.4 ± 3.8	-0.25 ± 2.8	-1290.4 ± 3.8
$Y_{0.5}Ca_{0.5}MnO_3$	-31.7 ± 3.6	9.4 ± 2.5	-1305.1 ± 3.6
$La_{0.5}Sr_{0.5}MnO_3$	-70.6 ± 5.6	-29.5 ± 2.2	-1294.2 ± 5.7
$La_{0.7}Sr_{0.3}MnO_3$	-69.1 ± 5.8	-44.4 ± 0.5	-1353.8 ± 5.9
$La_{0.9}Sr_{0.1}MnO_3$	-66.9 ± 5.9	-58.7 ± 1.9	-1412.7 ± 6.04

[a] Using the thermodynamic cycle involving AO, Ln_2O_3, Mn_2O_3, and O_2 (ΔH_{10}).
[b] Using the thermodynamic cycle involving AO, Ln_2O_3, Mn_2O_3, and MnO_2 (ΔH_{17}).

thermodynamic cycle used for $La_{1-x}Sr_xMnO_3$ is:

$$\Delta H_{12} \quad (1-x)/2\ La_2O_3\ (sol, 977\ K) + x\ SrO\ (sol, 977\ K) + (1-x/2)\ Mn_2O_3\ (sol, 977\ K) + x\ MnO_2\ (sol, 977\ K) \rightarrow La_{1-x}Sr_xMnO_3\ (s, 298\ K) \quad [12]$$

$$\Delta H_{13} \quad (1-x)/2\ La_2O_3\ (s, 298\ K) \rightarrow (1-x)/2\ La_2O_3\ (sol, 977\ K) \quad [13]$$

$$\Delta H_{14} \quad x SrO\ (s, 298\ K) \rightarrow x SrO\ (sol, 977\ K) \quad [14]$$

$$\Delta H_{15} \quad (1-x)/2\ Mn_2O_3\ (s, 298\ K) \rightarrow (1-x)/2\ Mn_2O_3\ (sol, 977\ K) \quad [15]$$

$$\Delta H_{16} \quad x MnO_2\ (s, 298\ K) \rightarrow x/2\ Mn_2O_3\ (sol, 977\ K) + x/4\ O_2\ (sol, 977\ K) \quad [16]$$

$$\Delta H_{17} \quad (1-x)/2\ La_2O_3\ (s, 298\ K) + x SrO\ (s, 298\ K) + (1-x)/2\ Mn_2O_3\ (s, 298\ K) + x MnO_2\ (g, 298\ K) \rightarrow La_{1-x}Sr_xMnO_3\ (s, 298\ K) \quad [17]$$

This cycle does not involve gaseous oxygen and there is no net change in oxidation state. The corresponding enthalpies of formation are reported in Table 5. The enthalpies of formation are more endothermic for the formation reaction without oxidation (ΔH_{17}) than for the one involving oxygen (see Fig. 2). Comparison of ΔH_{17} with ΔH_{10} allows the determination of the enthalpy of oxidation of Mn^{3+} to determination of the enthalpy of oxidation of Mn^{3+} to

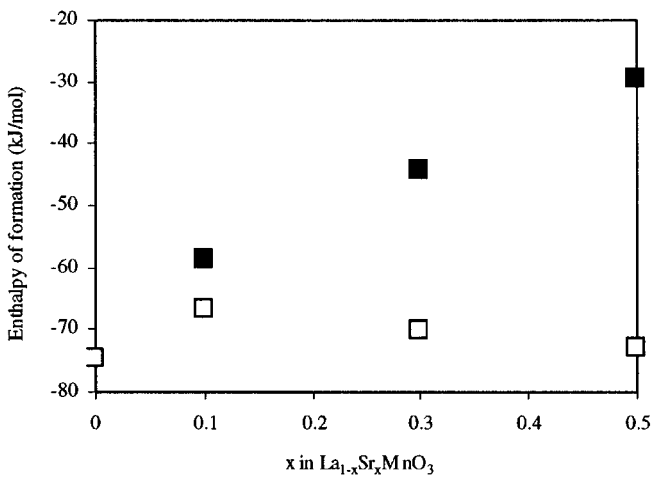

FIG. 2. Enthalpy of formation of $La_{1-x}Sr_xMnO_3$ perovskites as a function of the strontium content, x.

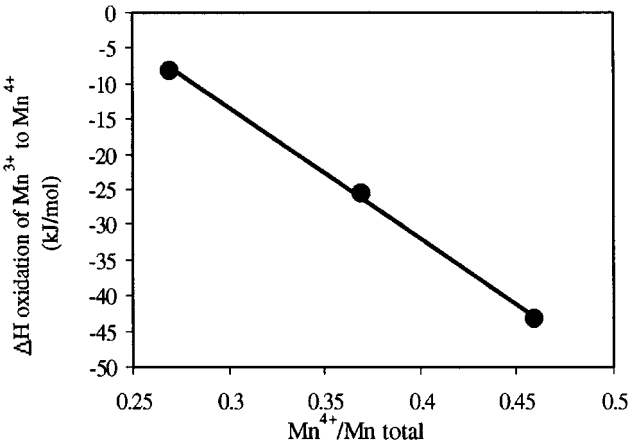

FIG. 3. Difference between enthalpy of formation involving Mn^{3+} oxidation (ΔH_9) and involving Mn_2O_3 and MnO_2 with no oxidation (ΔH_{16}) as a function of Mn^{4+} in the $La_{1-x}Sr_xMnO_3$ system.

difference between (ΔH_{17}–ΔH_{10}) as a function of Mn^{4+} in this system is shown in Fig. 3. This difference shows a linear trend with the Mn^{4+} content; the slope of the line represents the enthalpy of oxidation (Table 6), which is -184.7 ± 2.4 kJ/mol per mole of Mn^{4+}. This value is much more exothermic than the enthalpy of oxidation of 1/2 Mn_2O_3 to MnO_2 of -37.1 ± 7.0 kJ/mol of Mn (35). In the same manner, the enthalpies of oxidation of Mn^{4+} in the system $YMnO_3/Y_{0.5}Ca_{0.5}MnO_3$, $NdMnO_3/Nd_{0.5}Ca_{0.5}$ MnO_3, and $LaMnO_3/La_{0.5}Ca_{0.5}MnO_3$ have been evaluated. The value is 26.5 ± 2.4 kJ/mol for the yttrium system, -14.1 ± 2.5 kJ/mol for the neodynium system, and -76.5 ± 3.6 kJ/mol for the lanthanum system. The enthalpy of oxidation varies strongly with the nature of the A element and appears to become more exothermic as the parent trivalent cation gets larger (Y, Nd, La) and as the divalent dopant gets larger (Ca, Sr). This confirms qualitative ideas that larger cations stabilize high oxidation states (36).

For a given value of x, the amount of divalent doping, the enthalpy of formation varies with the nature of a divalent cation. $La_{0.5}Ca_{0.45}MnO_3$ is less stable in energy than $La_{0.5}Sr_{0.5}MnO_3$. A similar trend has been seen by DiCarlo *et al.* (36) for $La_{2-x}A_xCuO_{4-y}$ (A = Ba, Sr, Ca, Pb) and by Fritsch (34) for doped manganese dioxide. The enthalpy of oxidation of Mn^{3+} to Mn^{4+} depends on the nature of the A-site cation; the enthalpies become more negative with increasing basicity of the A cation.

Figure 4 shows the enthalpy of formation from an isochemical mixture of oxides of the perovskite, that is, ΔH for the reaction

$$\frac{1-x}{2} A_2O_3 (A = La, Nd, Y) + xA'O\ (A' = Sr, Ca) + \frac{1-x}{2} Mn_2O_3 + xMnO_2 \rightarrow A_{1-x}A'_xMnO_3. \quad [18]$$

TABLE 6
Enthalpy of Oxidation of Mn^{3+} to Mn^{4+} in Manganites

Compound	Mn^{4+}/Mn	ΔH_{10} (kJ/mol)[a]	ΔG_{17} (kJ/mol)[b]	$\Delta H_{17}-\Delta H_{10}$ (kJ/mol)	$\Delta H_{oxidation}$ kJ per mole Mn[c]
$LaMnO_3$	0	-74.8 ± 2.1	—	74.8 ± 2.1	
$La_{0.5}Ca_{0.5}MnO_3$	0.44	-56.6 ± 6.3	$-15.4 + 2.9$	41.2 ± 6.9	
					-76.5 ± 3.6
$YMnO_3$	0	-29.8 ± 2.1		28.8 ± 2.1	
$Y_{0.5}Ca_{0.5}MnO_3$	0.43	-31.8 ± 3.6	9.4 ± 2.5	41.2 ± 4.4	
					26.5 ± 2.4
$NdMnO_3$	0	-48.5 ± 1.8		48.5 ± 1.8	
$Na_{0.5}Ca_{0.5}MnO_3$	0.52	-41.4 ± 3.8	-0.25 ± 2.8	41.1 ± 4.7	
					-14.1 ± 2.5

[a] Enthalpy of formation of manganite using the thermodynamic cycle involving AO, Ln_2O_3, Mn_2O_3, and O_2 (ΔH_{10}).
[b] Enthalpy of formation of manganite using the thermodynamic cycle involving AO, Ln_2O_3, Mn_2O_3, and MnO_2 (ΔH_{17}).
[c] Enthalpy of oxidation of Mn^{4+} of manganite, obtained from the slope of the variation of the difference $\Delta H_{17}-\Delta H_{10}$ as a function of Mn^{4+}.

The set of data for $A = La$, $A' = Sr$ defines a straight line with doping content, allowing extrapolation to zero concentration of dopant to estimate the enthalpy of formation of $SrMnO_3$ at 295 K from SrO plus MnO_2 of 15.1 ± 0.9 kJ/mol. This value agrees with that inferred from thermogravimetric experiments (37). This positive enthalpy implies that $SrMnO_3$ is unstable with respect to SrO and MnO_2, since this solid state reaction, with no gas phase involved, would have a close to zero ΔS. The enthalpy of formation of $CaMnO_3$ can be estimated from an extrapolation of the three dotted lines in Fig. 4, taken from the La, Nd, and Y systems. They extrapolate to a common point, giving a heat of formation of 46.9 ± 5.8 kJ/mol. Thus, $CaMnO_3$ is even less stable than $SrMnO_3$, in accord with general trends that larger divalent cations are more effective in stabilizing high oxidation states for transition metals.

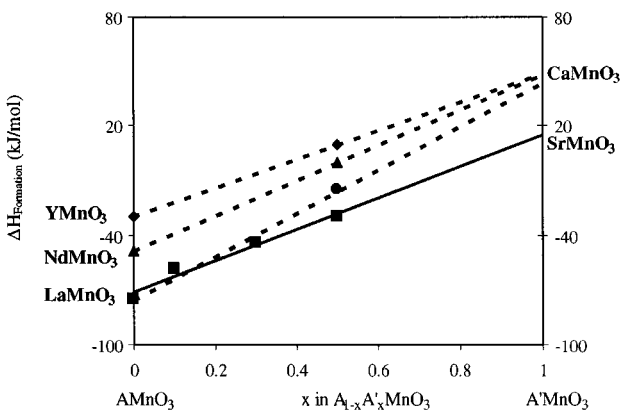

FIG. 4. Enthalpy of formation $1 - x/2\ A_2O_3 + xA'O + (1 - x)/2\ Mn_2O_3 + xMnO_2$ of $A_{1-x}A'_xMnO_3$ perovskite as a function of the divalent ion content, x. (■) $La_{1-x}Sr_xMnO_3$; (●) $La_{1-x}Ca_xMnO_3$; (▲) $Nd_{1-x}Ca_xMnO_3$; (◆) $Y_{1-x}Ca_xMnO_3$.'

At temperature above about 770 K, where MnO_2 is unstable, the equilibrium between $A'MnO_3$ and Mn_2O_3 must be considered:

$$A'O + \tfrac{1}{2}\,Mn_2O_3 + \tfrac{1}{4}\,O_2 \rightarrow A'MnO_3\,. \qquad [19]$$

For this reason, $\Delta H^\circ = -43.2 \pm 2.1$ kJ/mol for $CaMnO_3$ and -78.2 ± 0.9 kJ/mol for $SrMnO_3$. The entropy change for this reaction, which consumes O_2 gas, is negative. Thus, our data support the observation that $CaMnO_3$ and $SrMnO_3$ require intermediate temperatures and moderately high oxygen pressures for their syntheses. At too low temperatures, they may decompose (if kinetically allowed) to CaO (or SrO) + MnO_2, while at too high temperature they would probably disproportionate to phases containing trivalent manganese (e.g., $CaO + CaMn_2O_4$ or $SrO + SrMn_2O_4$).

Figure 5 shows the enthalpy relative to binary oxides (no oxidation involved) of $A_{1-x}A'_xMnO_3$ oxides, determined by calorimetric experiments. The enthalpy of formation of $LaMnO_3$ is more exothermic than that of $NdMnO_3$ by 26.3 kJ/mol and than that of $YMnO_3$ by 44.9 kJ/mol. Thus, the stability of the perovskite increases as the trivalent A-site cation increases in size.

However the substitution of a fraction of the trivalent (La, Nd, Y) by divalent cations (Sr, Ca) causes the enthalpy of formation to become less negative as the divalent cation content increases. The divalent cation content is directly related to the Mn^{4+} content, since these perovskites are essentially stoichiometric in oxygen. Thus, the enthalpy of formation from the oxides becomes less exothermic with increasing the Mn^{4+}/Mn^{3+} ratio. Analogous to the trend observed in $La_{1-x}Sr_xMnO_3$, the substitution of yttrium or neodynium by calcium in $YMnO_3$ increases the $Mn^{4+}/$

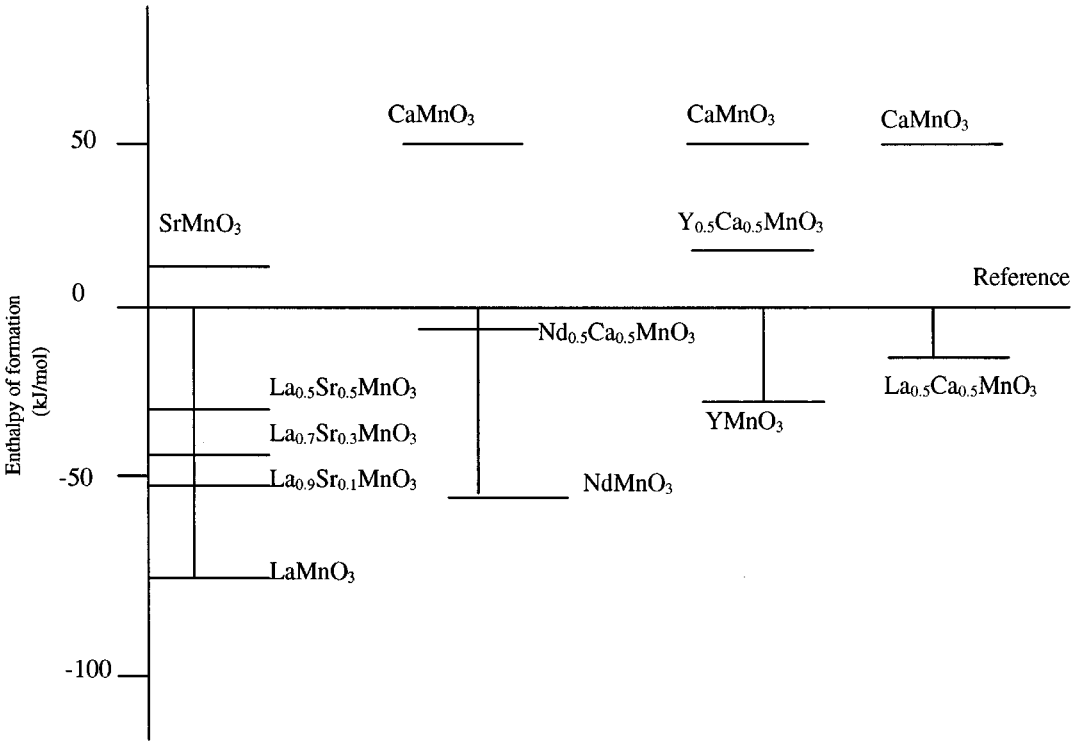

FIG. 5. Enthalpy relative to Mn_2O_3 and MnO_2 (and La_2O_3, Nd_2O_3, CaO, SrO) as needed of the perovskites studied. Reference of energy $(1-x/2)Mn_2O_3 + xMnO_2 + (1-x/2)\,Ln_2O_3 + xAO$ with Ln = La, Nd and A = Ca, Sr.

Mn^{3+} ratio and destabilizes the structure. Thus, $A_{0.5}Ca_{0.5}MnO_3$ has a less negative enthalpy of formation from the oxides than $AMnO_3$, where all the manganese is in the 3+ oxidation state. $CaMnO_3$ (with all Mn tetravalent) is the least stable energetically.

PHASE DIAGRAM OF THE La–Mn–O SYSTEMS

The new values of enthalpies of oxidation determined by calorimetry and reliable standard entropies taken from the literature were used to obtain the phase diagram for the La–Mn–O system. The standard state free energy ΔG°_T is given by the relation

$$\Delta G^\circ_T = \Delta H^\circ_T - T\Delta S^\circ_T = -RT\ln K, \qquad [20]$$

where ΔH°_T is the standard state enthalpy change, ΔS°_T, the standard entropy change, R is the gas constant, T is the absolute temperature, and K is the equilibrium constant.

Assuming that the solid phases in the system are pure, the activity of the solid phase is equal to 1, so $K = P^n_{O_2}$, for the reactants and products of reactions, Eq. [20] can be written as

$$LaMnO_3 \rightarrow \tfrac{1}{2}Mn_2O_3 + \tfrac{1}{4}O_2 + \tfrac{1}{2}La_2O_3 \qquad [21]$$

$$LaMnO_3 + \tfrac{1}{4}O_2 \rightarrow MnO_2 + \tfrac{1}{2}La_2O_3 \qquad [22]$$

$$\Delta G^\circ_T = -1/4\ RT\ \mathrm{In}\,P_{O_2} \text{ for equilibrium [21]} \qquad [23]$$

$$\Delta G^\circ_T = +1/4\ RT\ \mathrm{In}\,P_{O_2} \text{ for equilibrium [22]} \qquad [24]$$

The variation of the standard free energy with temperature is expressed in the form

$$A'O + \tfrac{1}{2}Mn_2O_3 + \tfrac{1}{4}O_2 \rightarrow A'MnO_3. \qquad [25]$$

For the reactants and products of reactions [21] and [22], the molar heat capacity C_P is expressed over a range of temperature as

$$\Delta C_P = \Delta a + \Delta bT + \Delta cT^2. \qquad [26]$$

Thus, the integral terms in Eq. [26] have been calculated for reactions Eqs. [21], [22]. The heat capacity, C_P, equations are from Ref. (38) for MnO, Ref. (38) for La_2O_3, and Refs. (39) and (40) for $LaMnO_3$. The standard entropy for MnO, MnO_2, La_2O_3, and O_2 has been taken from the thermodynamic tables of Robie and Hemingway (27). For $LaMnO_3$, the standard entropy values have been estimated from Schumm *et al.* (41). The Gibbs free energies of formation

TABLE 7
The Enthalpies and Gibbs Free Energies of Formation from the Oxides for $LaMnO_3$ from $T = 300$ K to $T = 1100$ K

Reaction	T (K)	$\Delta H^\circ_{T\,298}$ (kJ/mol)	$\Delta S^\circ_{T\,298}$ ($J.mol^{-1}.K^{-1}$)	$\Delta G^\circ_{T\,298}$ (kJ/mol)
$4LaMnO_3 + O_2 \rightarrow 4MnO_2 + 2LaO_3$				
	300	128.98	− 221.71	195.49
	400	131.27	− 215.45	217.45
	500	137.82	− 200.99	238.32
	600	147.94	− 182.65	257.53
	700	161.81	− 161.35	274.75
	800	179.91	− 137.24	289.71
	900	202.88	− 110.25	302.10
	1000	231.41	− 80.25	311.65
	1100	266.23	− 47.10	318.05
$4LaMnO_3 \rightarrow 4MnO + 2La_2O_3 + O_2$				
	300	650.38	216.59	585.40
	400	653.27	203.29	571.95
	500	658.94	199.22	559.33
	600	667.52	201.19	546.80
	700	679.51	208.13	533.82
	800	695.58	219.57	519.92
	900	716.43	235.31	504.65
	100	742.83	255.22	487.61
	1100	775.54	279.25	468.36

from the oxides for $LaMnO_3$, from $T = 300\,K$ to $T = 1100\,K$ are given in Table 7, with $\Delta H^0_{T\,298}$ and $\Delta S^0_{T\,298}$ for each reaction.

The variation of $\log P_{O_2}$ with T can be deduced by applying the relation

$$\log P_{O_2} = \pm \frac{\Delta G^\circ_T}{R \ln 10} \times \frac{1}{T}. \qquad [24]$$

The calculated $LaMnO_3/MnO$ phase boundary (Fig. 6) of the present study agrees reasonably with that of Atsumi *et al.* (37). The agreement between calorimetric data and the P_{O_2} measurement confirms the consistency of direct calorimetric experiments and also suggests that equilibrium was indeed maintained in the P_{O_2} measurements and that the $LaMnO_3$ phase did not vary significantly in stoichiometry. The calculated phase stability diagram of the manganese–oxygen system, using the calorimetric values of Fritsch (35), is also shown in Fig. 6. The introduction of lanthanum involves a shift to higher temperature of the boundary between Mn^{3+}/Mn^{4+}, compared to boundaries in the Mn–O system, which reflects the stabilizing effect of the lanthanum for the perovskite phase containing Mn^{3+}, namely, $LaMnO_3$.

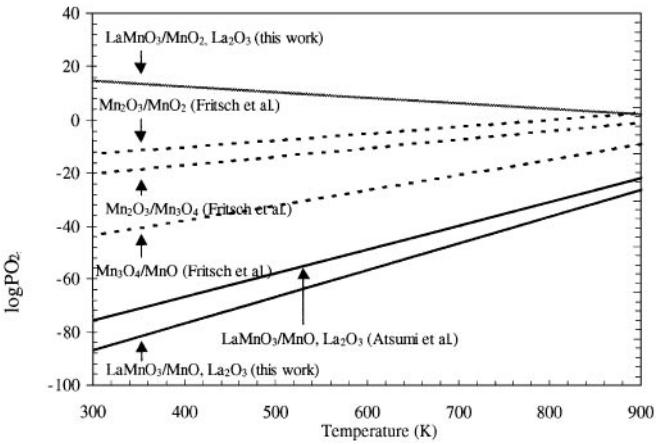

FIG. 6. Equilibrium in the manganese–oxygen system and lanthanum–manganese–oxygen system.

CONCLUSIONS

The energetics of $LaMnO_3$, $YMnO_3$, $NdMnO_3$, $La_{1-x}Sr_xMnO_3$ (with $0.1 < x < 0.9$), and $A_{1-x}Ca_xMnO_3$ (with A = La, Nd, Y) systems has been determined by high temperature drop solution calorimetry. It has been established that the stability of the perovskite structure depends on the size of the A-site cations. A comparison of the enthalpies of formation of $A_{0.5}Ca_{0.5}MnO_3$ perovskites shows that the stability of the structure increases with the size of the trivalent element in the A site. The nature of the divalent dopant also affects the energetics. The more basic (and larger) A-site cation is associated with the more negative enthalpy of formation and the more negative enthalpy of oxidation of Mn^{3+} to Mn^{4+}.

The phase stability diagram of the lanthanum–manganese–oxygen system in the temperature range 300–1100 K has been plotted using the values of the enthalpies of oxidation. The shift to higher temperature of the boundary between Mn^{3+}/Mn^{4+} in the La–Mn–O system, compared to the Mn–O system, reflects the stabilizing effect of lanthanum for the phase containing Mn^{3+}, namely perovskite.

ACKNOWLEDGMENTS

This work was supported by the National Science Foundation (Grant DMR-9703922). The authors thank Anthony Cheetham for helpful discussion.

REFERENCES

1. K. Chahara, T. Ohno, M. Kasai, and Y. Kozono, *Appl. Phys. Lett.* **63,** 1990 (1993).
2. A. Urushibara, Y. Moritomo, T. Arima, A. Asamitsu, G. Kido, and Y. Tokura, *Phys. Rev. B* **51,** 14103 (1995).
3. R. Mahendiran, R. Mahesh, N. Rangavittal, S. K. Tiwari, A. K. Raychaudhuri, T. V. Ramaskrishnan, and C.N.R. Rao, *Phys. Rev. B* **53,** 3348 (1996).

4. B. Raveau, A. Maignan, and V. Caignaert, *J. Solid State Chem.* **117,** 424 (1995).
5. J. A. M. van Roosmalen, E. H. P. Cordfunke, R. B. Helmholdt, H. V. Zandbergen, *J. Solid State Chem.* **110,** 100 (1994).
6. J. A. M. van Roosmalen, J. P. P. Huijsmans, and L. Plomp, *Solid State Ionics* **66,** 279 (1993).
7. R. Mahendiran, S. K. Tiwary, A. K. Raychaudhuri, T. V. Ramakrishnan, R. Mehesh, N. Rangavittal, C. N. R. Rao. *Phys. Rev B* **53,** 3348 (1996).
8. Y. Takeda, R. Kanno, M. Noda, and O. Yamomoto, *Bull. Inst. Chem. Rew.* **64,** No. 4, 157 (1986).
9. S. C. Singhal, R. J. Ruka, S. Sinharoy, "Interconnection Materials Development for Solid Fuel Cells," Westinghouse R&D Center, Pittsburgh, Pennsylvania, 1985.
10. L. W. Tai, P. A. Lessing, *J. Am. Ceram. Soc.* **74,** No. 1, 155 (1991).
11. O. Yamomoto, Y. Takeda, R. Kanno, and M. Noda, *Solid State Ionics* **22,** 241 (1987).
12. M. L. Bordera and F. Abbattista, *J. Less. Common Met.* **92,** 55 (1983).
13. N. Kamegashira and Y. Hiyoski, *Mat. Lett.* **2,** 337 (1984).
14. O. M. Sreedharan, R. Pankajavalli, and J. B. Gnanamoorthy, *High Temp. Sc.* **16** (1983).
15. K. Kamata, T. Nakajina, T. Hayashi and T. Nakamura, *Mater. Res. Bull.* **13,** 49, 251 (1978).
16. T. Nakamura, G. Petzow and L. J. Gauckler, *Mater. Res. Bull.* **14,** 649 (1979).
17. N. Kamegashira, Y. Miyazaki and Y. Hiyoshi, *Mater. Lett.* **3,** 194 (1984).
18. O. M. Sreedharan, R. Pankajavalli, and J. B. Gnanamoorthy, *Mater. Lett.* 2, **6A, B** (1984).
19. S. Fritsch, A. Navrotsky, Private Communication, 1997.
20. C. N. R. Rao, A. K. Cheetham, R. Mahesh, *Chem. Mater.* **8,** 2421 (1996).
21. R. Mahesh, R. Mahendiran, A. K. Raychaudhuri, C. N. R. Rao, *J. Solid State Chem.* **114,** 297 (1995).
22. A. Navrotsky, *Phys. Chem. Miner.* **2,** 89 (1977).
23. A. Navrotsky, *Phys. Chem. Miner.* **24,** 222 (1997).
24. A. Navrotsky, *MRS Spring Meeting Symp. S. Proc.* **432,** 3 (1997).
25. R. D. Shannon, *Acta Cryst. A* **32,** 751 (1976).
26. J. M. McHale, A. J. Perrotta, and A. Navrotsky, *J. Phys. Chem. B* **101,** 603 (1997).
27. R. A. Robie and B. S. Hemingway, *US Geol. Surv. Bull.* **1456,** 456 (1995).
28. J. Bularzik, A. Navrotsky, J. DiCarlo, J. Bringley, B. Scott, and S. Trail, *J. Solid State Chem.* **93,** 418 (1991).
29. E. Takayama-Muromachi and A. Navrotsky, *J. Solid State Chem.* **106,** 349 (1993).
30. Z. Zhou and A. Navrotsky, *J. Mater. Res.* **7,** 2920 (1992).
31. L. Chai and A. Navrotsky, *Geochim. Cosmochim. Acta* **59,** 939 (1995).
32. E. Takayama-Muromachi and A. Navrotsky, *J. Solid State Chem.* **72,** 244 (1988).
33. R. Mahesh, K. R. Kannan, and C. N. R. Rao, *J. Solid State Chem.* **114,** 294 (1995).
34. S. Fritsch, E. J. Post, S. L. Suib, and A. Navrotsky, *Chem. Mater.* **61,** 13, 2613 (1998).
35. S. Fritsch and A. Navrotsky, *J. Am. Ceram. Soc.* 79, **7,** 1761 (1996).
36. J. DiCarlo, J. Bularzik, and A. Navrotsky, *J. Solid State Chem.* **96,** 381 (1992).
37. T. Atsumi, T. Ohgushi and N. Kamegashira, *J. Alloys Compounds* **238,** 35 (1996).
38. J. H. Kuo, H. U. Anderson, and D. M. Sparlin, *J. Solid State Chem.* **87,** 55 (1990).
39. K. Kinukawa, M. Takagi, H. Satoh, and N. Kamegashira, *Kidorui* **30,** 132 (1997).
40. M. Takagi, K. Kinukawa, H. Satoh, and N. Kamegasira, *Kidorui* **28,** 110 (1996).
41. R. H. Schumm, D. D. Wagman, S. Bailey, W. H. Evans, and V. B. Parker, *U.S. Natl. Bur. Standards Tech. Note* **270-7,** 75 (1973).